5
Nonlocal correlations and efficiencies of partially entangled three qubit states

5.1 INTRODUCTION

To identify nonlocal correlations existing in quantum systems, reliable operators have been presented in previous two chapters. Those nonlocal correlations are fundamental resources for quantum information processing such as quantum teleportation [Bennett *et al.*, 1993], quantum cryptography [Gisin *et al.*, 2002], quantum computing [Steane, 1998] etc. Next part of the Thesis analyzes efficacies of partially entangled states for different quantum information processing protocols. The next two chapters readdress the question of usefulness and efficiency of multi-qubit partially entangled states under real noisy conditions using weak measurement and its reversal operations. For this purpose, present chapter analyzes and compares efficiencies of four different sets of three-qubit partially entangled states from two inequivalent classes, namely $|GHZ\rangle$ (Greenberger-Horne-Zeilinger) class and $|W\rangle$ class [Dür *et al.*, 2000], for teleportation and dense coding protocols. The analysis in this chapter shows some interesting observations regarding applications of weak measurement and its reversal operations for amplitude damping channels. For instance, using a class of ($|\Phi\rangle$) states belonging to the $|GHZ\rangle$ class as resources for quantum teleportation, the fidelity of teleportation is always close to unity for higher values of the weak measurement strength parameter irrespective of the strengths of noise and the state parameter θ. For $|GHZ\rangle$ and $|W\rangle$ classes of states, applications of weak measurements lead to an increase in the fidelity of teleportation compared to that in the presence of noise alone. A comparison of these results suggests that for lower values of state parameter θ, the $|\Phi\rangle$ states are much more robust to decoherence in comparison to other generalized-GHZ ($|GGHZ\rangle$) states; whereas for higher values of θ, $|GGHZ\rangle$ states are more robust in comparison to $|\Phi\rangle$ states. In general, $|\Phi\rangle$ and $|GGHZ\rangle$ states are always more robust to noise in comparison to $|W\rangle$ states. The results further suggest that more entanglement and nonlocal correlation in the input state may not always lead to better efficiency in a protocol in presence of noise and weak measurements, i.e., in certain cases one may identify partially entangled input state to be more efficient than the maximally entangled input state.

For characterizing quantum correlations in the finally shared three-qubit states, this chapter uses three-qubit Svetlichny inequality [Svetlichny, 1987] whose violation is a necessary and sufficient condition to confirm the presence of nonlocal correlations in an underlying quantum state. The results indicate that although the Svetlichny inequality is not violated by three-qubit partially entangled states even for small decoherence parameter, the fidelity of teleportation is surprisingly greater than $\frac{2}{3}$. A further comparison of efficiencies of these states for dense coding protocol under similar scenarios lead to similar results as in the case of teleportation protocol, i.e., $|\Phi\rangle$ states are found to be more efficient in comparison to $|GGHZ\rangle$ states for smaller values of the state parameter θ, and $|\Phi\rangle$ and $|GGHZ\rangle$ states are always more efficient than $|W\rangle$ states. In addition to the Svetlichny inequality, quantum correlations in these three-qubit states are also characterized using the modified Mermin inequality presented in Chapter 3 and using global quantum discord [Rulli and Sarandy, 2011]. Unlike the Svetlichny inequality, modified Mermin inequality and global quantum discord identify nonlocal correlations in these states even in presence of decoherence. This further explains the robustness of nonlocal correlations in these states and their efficiencies in the region where the Svetlichny inequality fails to identify nonlocal

correlations.

The efficiencies of partially entangled three-qubit states for communication protocols is analyzed using an optimal relation between weak measurement parameter, weak measurement reversal parameter and decoherence parameter. Interestingly, with the application of non-optimum reversing weak measurement, for a fixed value of the decoherence parameter, the partially entangled $|GGHZ\rangle$ states are more efficient for quantum information protocols than all other states of the same class, for certain values of weak measurement operations. For example, at $d = 0.5$, for a fix value of weak measurement reversal parameter as 0.99, the use of partially entangled $|GGHZ\rangle$ states as resources result in very high teleportation fidelity at very small values of state parameter $\theta \in [.003, .4]$, for all values of weak measurement strength below 0.98. Therefore, the results in this chapter indicate that states with less initial correlations may also prove to be more useful in comparison to states with higher initial correlations under noisy conditions suggesting that higher initial correlations may not always guarantee higher success in a communication protocol. Hence, the efficiency of a set of states depends on different parameters, i.e., the state parameter, noise parameter, weak measurement and its reversal operations (optimal and non-optimal)- the values of these parameters decide whether to use a $|\Phi\rangle$ or a $|GGHZ\rangle$ state in real conditions. Thus, depending on the analysis presented in this chapter, one can use an appropriate state as a resource in an actual protocol set-up to obtain the maximum efficiency. The study presented here can be useful to researchers working in theory as well as experiments.

The rest of the chapter is organized as follows: Section 5.2 shows nonlocal correlations of partially entangled states using Svetlichny and Mermin-cumulant inequalities. The efficiencies of partially entangled states for teleportation protocol in the presence of noise and with the application of weak measurements are discussed in Section 5.3. The discussion on quantum dense coding protocol using partially entangled three-qubit states is presented in Section 5.4. Efficiencies of partially entangled states in noisy conditions using non-optimum weak measurement operations are described in Section 5.5. Finally, Section 5.6 summarizes the chapter.

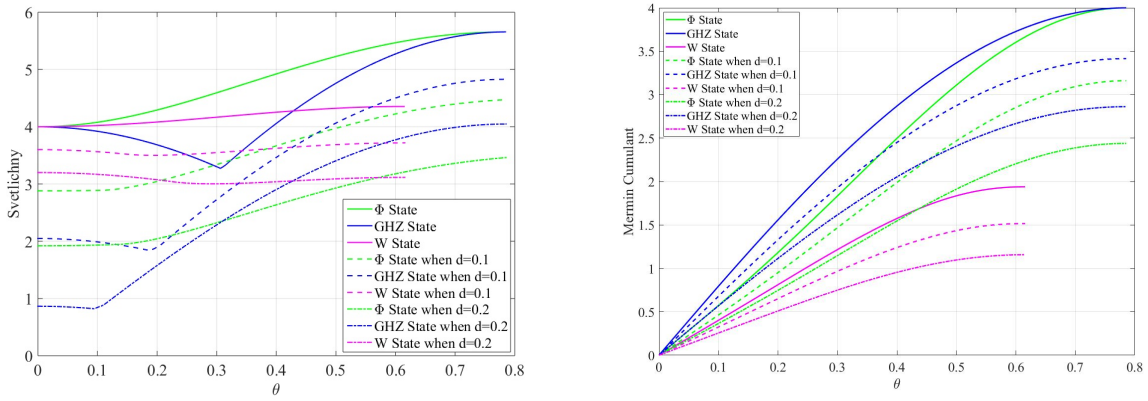
5.2 NONLOCAL CORRELATIONS

Quantum theory allows correlations between spatially separated particles that are fundamentally different from classical correlations. For example, the violation of Bell-type inequalities in two-qubit and multi-qubit entangled systems confirms the presence of genuine quantum correlations between qubits. These correlations, when subjected to noisy quantum channels, degrade due to decoherence, adversely affecting the overall efficiency of a protocol. In this chapter, we focus on analyzing nonlocal correlations in three-qubit systems in presence of noise and then address the question of efficiencies of partially entangled three-qubit states under real situations.

For three-qubit systems, the local hidden variable theories suggest that all product and bi-separable states must satisfy the Svetlichny inequality [Svetlichny, 1987], defined as

$$|S| = A(BC + BC' + B'C + B'C') + A'(BC + BC' + B'C + B'C') \leq 4 \tag{5.1}$$

where $A = \vec{a}.\vec{\sigma}_a$ or $A' = \vec{a'}.\vec{\sigma}_a$ are measurements performed on the first sub-system; similarly, $B = \vec{b}.\vec{\sigma}_b$ or $B' = \vec{b'}.\vec{\sigma}_b$ and $C = \vec{c}.\vec{\sigma}_c$ or $C' = \vec{c'}.\vec{\sigma}_c$ are measurements performed on second and third sub-systems respectively. Here $\vec{\sigma}_i = \{\sigma_x, \sigma_y, \sigma_z\}$ (with $i = a, b, c$) are spin projection operators, and $\vec{a}$, $\vec{b}$, $\vec{c}$, $\vec{a'}$, $\vec{b'}$, $\vec{c'}$ are unit vectors in $\mathbb{R}^3$, given as $\vec{a} = (Sin\theta_a Cos\phi_a, Sin\theta_a Sin\phi_a, Cos\theta_a)$. The unit vectors $\vec{b}$, and $\vec{c}$ can be defined in a similar fashion; and $\vec{a'}$, $\vec{b'}$, $\vec{c'}$ can represented in an equivalent way with primes on angles.
Therefore, the Svetlichny inequality confirms the presence of genuine tripartite correlations between qubits. In general, the violation of Svetlichny inequality, thus, suggests that the



(a) (b)

Figure 5.1 : Effects of decoherence on quantum correlations using the (a) Svetlichny inequality, (b) proposed Mermin-cumulant inequality for $|\Phi\rangle$, $|GGHZ\rangle$ and $|W\rangle$ states

underlying quantum state can be used as an efficient resource in quantum information processing. For example, the Svetlichny inequality is violated by the three-qubit state $|\Phi\rangle = \frac{1}{\sqrt{2}}[Cos\theta(|000\rangle + |011\rangle) + Sin\theta(|110\rangle - |101\rangle)]$ for the whole range of parameter θ or by the set of $|GGHZ\rangle$ states, i.e., $|GGHZ\rangle = Cos\theta\,|000\rangle + Sin\theta\,|111\rangle$ for $\theta > 0.4rad.$, and hence $|\Phi\rangle$ and $|GGHZ\rangle$ states can be considered as useful resources for quantum information and computation, at least in the ideal scenario, i.e., in the absence of noise. However, as shown in Figure 5.1(a), the inequality is not violated by $|\Phi\rangle$ states even if the decoherence parameter is as small as 0.2. Here we consider the amplitude damping channel as an example of a noisy channel assuming that all three qubits pass through the noise of equal strength. In fact, even for $d = 0.1$, the inequality is violated only by a smaller set of states, where d is the amplitude damping noise parameter. Figure 5.1(a), therefore, suggests that although $|\Phi\rangle$ states always violate the Svetlichny inequality in ideal conditions, the nonlocal correlations in these states degrade very fast when exposed to real conditions. Similar to $|\Phi\rangle$ states, $|GGHZ\rangle$ states also do not violate the inequality if the decoherence parameter is greater than 0.2. Precisely, even for the value of decoherence parameter as small as 0.2, only a fraction of states violate the Svetlichny inequality. Interestingly, for $d = 0.1$, the violation of Svetlichny inequality by $|GGHZ\rangle$ states is more prominent than $|\Phi\rangle$ states, i.e., although $|\Phi\rangle$ states violate the Svetlichny inequality more in comparison to $|GGHZ\rangle$ states in ideal conditions, the $|GGHZ\rangle$ states exhibit more nonlocal correlations in comparison to $|\Phi\rangle$ states under mild noisy conditions. In comparison to $|GGHZ\rangle$ and $|\Phi\rangle$ states; $|W\rangle$ states, i.e., $|W\rangle = Sin\theta\,|001\rangle + Cos\theta(|100\rangle + |010\rangle)/\sqrt{2}$, do not reveal presence of nonlocal correlations even at $d = 0.1$.

In addition to the Svetlichny inequality, we have also analyzed nonlocal correlations in three-qubit partially entangled states using Mermin-cumulant inequality discussed in Chapter 3. The Mermin-cumulant inequality (Eq. (3.2)) in the Chapter 3 is defined as a modification to the existing Mermin inequality, given as

$$|M_{cum}| = |E(ABC)_{cum} - E(AB'C')_{cum} - E(A'BC')_{cum} - E(A'B'C)_{cum}| \leq 0 \tag{5.2}$$

where

$$E(ABC)_{cum} = E(ABC) - E(A)E(BC) - E(B)E(AC) - E(C)E(AB) + 2E(A)E(B)E(C)$$

and $E(AB'C')_{cum}$, $E(A'BC')_{cum}$ and $E(A'B'C)_{cum}$ are defined in a similar fashion. The upper bound of this inequality consistent with the local correlations in pure three-qubit states is 0. Figure 5.1(b) shows the violation of proposed inequality for $|GGHZ\rangle$, $|\Phi\rangle$ and $|W\rangle$ states in the presence of noise.

In comparison to $|GGHZ\rangle$ states, the optimum value of Mermin-cumulant operator for $|\Phi\rangle$ states decrease rapidly in the noisy environment. Although the inequality shows violation for all three states in the presence of noise, the violation decreases significantly with increasing noise. For higher values of noise parameter, the violation of Mermin-cumulant inequality is significantly low, i.e., close to the classical limit. Considering the inevitability of noise and vulnerability of nonlocal correlations in partially entangled three-qubit states even in presence of mild noise, the analysis of efficiency of such states under real noisy conditions requires adequate attention. Hence, in the next few sections, we discuss and analyze the efficiencies of partially entangled three-qubit states under real conditions.

5.3 QUANTUM TELEPORTATION USING QUANTUM GATES

Quantum teleportation [Bennett *et al.*, 1993] is a process which allows a sender to communicate an unknown quantum information to a sender with the help of a shared entangled resource without sending the encoded information physically through a medium. In order to facilitate the discussion regarding our results, we first briefly describe quantum teleportation - Alice (sender) and Bob (receiver) share an entangled state $|\psi_{23}^{-}\rangle$, which acts as a quantum channel for the teleportation protocol. Alice wants to send an unknown information encoded in a state $|\psi_{in}\rangle = Cos(\xi/2)|0\rangle + e^{\iota\phi}Sin(\xi/2)|1\rangle$ to Bob, where ξ and ϕ are polar coordinates of a three-dimensional unit sphere known as Bloch sphere with $0 \leq \xi \leq \pi$ and $0 \leq \phi \leq 2\pi$. For this, Alice first performs a two-qubit Bell-state measurement on the joint state of her qubits- one from the shared entangled pair and one defining the input state, and then sends the measurement outcomes to Bob through a classical channel. Bob, then performs a unitary transformation to retrieve the unknown input state, which is destroyed at Alice's end.

As a criterion for successful teleportation, one can compute teleportation fidelity which indicates the degree of overlap between input and output states. For example, fidelity of quantum teleportation can be expressed as the overlap of input state $|\psi_{in}\rangle$ and output state ρ_{out} as

$$F = \langle\psi_{in}|\rho_{out}|\psi_{in}\rangle \tag{5.3}$$

Since the initial state is unknown, the average fidelity [Massar and Popescu, 1995] can also be given as,

$$F_{avg} = \frac{1}{4\pi}\int_0^{2\pi} d\phi \int_0^{\pi} FSin(\xi)d\xi \tag{5.4}$$

5.3.1 Three qubit states as quantum channels for teleportation under real conditions

In order to analyze efficiencies of partially entangled multi-qubit states in terms of teleportation fidelity in the noisy environment, we now proceed to study four different sets of three-qubit states belonging to two inequivalent classes. As discussed above, for our purpose we consider four different sets of states, namely, $|\Phi\rangle$ states, $|GGHZ\rangle$ states, $|W\rangle$ states and $|W_n\rangle$ states.

$|\Phi\rangle$ *states as quantum channels under real conditions*

First, we consider partially entangled $|\Phi\rangle$ states as a channel for teleportation protocol where

$$|\Phi\rangle = \frac{1}{\sqrt{2}}[Cos\theta(|000\rangle + |011\rangle) + Sin\theta(|110\rangle - |101\rangle)] \tag{5.5}$$

As an example, Figure 5.2 demonstrates the proposed quantum circuit for teleporting an unknown information encoded in the state $|\psi_{in}\rangle = \alpha|0\rangle + \beta|1\rangle$, where α and β are real numbers and $\alpha^2 + \beta^2 = 1$, using $|\Phi\rangle$ state as a quantum channel under ideal conditions. Here H, X and Z

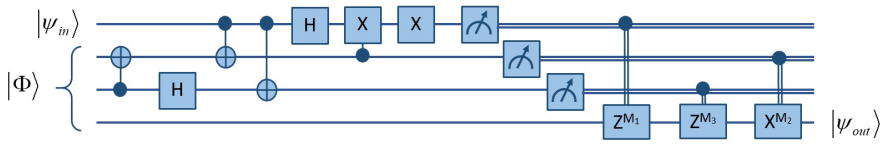


Figure 5.2 : A quantum circuit for teleportation using the $|\Phi\rangle$ state as a quantum channel

represent Hadamard, Pauli X and Pauli Z operations, respectively and the two-qubit operations are Controlled-NOT (C-NOT), Controlled-X and Controlled-Z operations.
Using the teleportation circuit diagram in Figure 5.2, $|\psi_{out}\rangle$ can be evaluated as

$$|\psi_{out}^{(1)}\rangle = \frac{1}{2\sqrt{2}}\left(\frac{(Cos\theta + Sin\theta)(\alpha|0\rangle + \beta|1\rangle)}{\sqrt{p(\psi_{out}^{(1)})}}\right) \text{ or } |\psi_{out}^{(2)}\rangle = \frac{1}{2\sqrt{2}}\left(\frac{(Cos\theta - Sin\theta)(\alpha|0\rangle + \beta|1\rangle)}{\sqrt{p(\psi_{out}^{(2)})}}\right)$$

depending on whether the measurement outcomes of first three qubits is $(000, 100, 011, 111)_{123}$ or $(001, 101, 010, 110)_{123}$, respectively. Considering $p(\psi_{out}^{(i)})$ are probabilities associated with measurement outcomes $|\psi^{(i)}\rangle$ such that $p(\psi_{out}^{(1)}) = \frac{1}{8}(Cos\theta + Sin\theta)^2$ and $p(\psi_{out}^{(2)}) = \frac{1}{8}(Cos\theta - Sin\theta)^2$. Therefore, using the obtained outputs and Eq. (5.3), fidelity can be calculated as

$$F^{(1)} = \frac{1}{8}\left(\frac{(\alpha^2+\beta^2)^2(Cos\theta + Sin\theta)^2}{p(\psi_{out}^{(1)})}\right) \text{ or } F^{(2)} = \frac{1}{8}\left(\frac{(\alpha^2+\beta^2)^2(Cos\theta - Sin\theta)^2}{p(\psi_{out}^{(2)})}\right), \text{ respectively.}$$

Hence, the average fidelity $F_{avg} = \sum_i p(\psi_{out}^{(i)})F^{(i)}$ can be given as

$$F_{avg} = \frac{1}{2}[(C_\theta + S_\theta)^2 + (C_\theta - S_\theta)^2](\alpha^2+\beta^2)^2 = 1 \tag{5.6}$$

where $C_\theta = Cos\theta$ and $S_\theta = Sin\theta$. Clearly, the average teleportation fidelity in this case is found to be 1 indicating a perfect teleportation and showing that the fidelity of teleportation is independent of the state parameter θ. The unit fidelity can be attributed to the properties of $|\Phi\rangle$ states, however, we are interested in the efficiency or usefulness of these states under noisy conditions. Therefore, we now consider the teleportation protocol in a decoherence environment, i.e., using amplitude damping channels. The single-qubit amplitude damping Kraus operators, defined in Eq. (1.44) of Chapter 1, operate on the individual qubits such that the state now evolves as $\varepsilon(\rho)$. Since the initial state after operations of amplitude damping channels evolves as a mixed state, therefore, the three-qubit input state in Figure 5.2 is now a three-qubit mixed state instead of a three-qubit pure state. Considering all three qubits of the state $|\Phi\rangle$ to suffer from decoherence, the average fidelity can be expressed as

$$F_{avg}^{(d)} = \frac{1}{6}\{4 + 2\sqrt{\bar{d}_2}\sqrt{\bar{d}_3} - d_2\bar{d}_3 - d_3\bar{d}_1 + d_1(-\bar{d}_2 - 2\sqrt{\bar{d}_2}\sqrt{\bar{d}_3}) + (2d_1\sqrt{\bar{d}_2}\sqrt{\bar{d}_3} + d_2d_3 + d_1(\bar{d}_2 - d_3))C_{2\theta}\} \tag{5.7}$$

where d_1, d_2, and d_3 are the amplitude damping noise parameters associated with qubits 1, 2 and 3, respectively ($0 \leq d_1 \leq 1$, $0 \leq d_2 \leq 1$, and $0 \leq d_3 \leq 1$) and $\bar{d}_i = 1 - d_i$. Eq. (5.7) indicates that teleportation fidelity decreases with the increasing value of amplitude damping noise parameter (see Figure 5.3(a)). Surprisingly, in this case, teleportation fidelity using the finally shared state is always more if the initially prepared state is a partially entangled state instead of a maximally entangled state. Evidently, lesser the entanglement of the initial state, more is the teleportation fidelity. Therefore, partially entangled $|\Phi\rangle$ states are more robust towards amplitude damping noise in comparison to the maximally entangled $|\Phi\rangle$ state, as far as the average fidelity is concerned. The above observation further suggests that maximum nonlocality and entanglement in the initial state may not always guarantee maximum efficiency in presence of noise [Acin *et al.*, 2002a; Méthot and Scarani, 2007; Hiesmayr, 2007; Brunner, 2010; Junge and Palazuelos, 2011; Vidick and Wehner, 2011; Chaves *et al.*, 2014; de Rosier *et al.*, 2017; Singh and Kumar, 2018b]. In fact, for very strong

decoherence, the maximally entangled state may not even lead to a fidelity $> \frac{2}{3}$ as shown in Figure 5.3(a) and Figure 5.3(b). Hence, more nonlocal correlations in the initial state do not always lead to optimal success in a given protocol. Interestingly, even though $|\Phi\rangle$ states do not violate the three-qubit Svetlichny inequality for $d \geq 0.2$, the average fidelity using these states is still $> \frac{2}{3}$ for $d \geq 0.2$. In fact, under the influence of strong decoherence also, the average fidelity still exceeds the classical limit for certain ranges of the state parameter θ. On the other hand, $|\Phi\rangle$ states violate modified Mermin and Svetlichny inequalities for these values of the noise parameter as discussed in Chapter 3 indicating the reasons for the efficiency of these states in presence of noise.

We further analyze the efficiency of $|\Phi\rangle$ states using the applications of weak measurements and its reversal operations as depicted in Figure 1.3. The average teleportation fidelity after a sequence of weak measurements, amplitude damping channels and quantum measurement reversal operations is evaluated as

$$F_{avg}^{(w)} = \frac{2}{3}\left[\frac{6+d_3\bar{w}_3(1+d_1\bar{w}_1)+d_2\bar{w}_2(1+d_1\bar{w}_1+d_3\bar{w}_3)-(d_1\bar{w}_1(d_2\bar{w}_2+d_3\bar{w}_3)-d_2d_3\bar{w}_2\bar{w}_3)C_{2\theta}}{(2+d_2\bar{w}_2)(2+d_3\bar{w}_3)+d_1\bar{w}_1(2+d_2\bar{w}_2+d_3\bar{w}_3)-(d_1\bar{w}_1(2+d_2\bar{w}_2+d_3\bar{w}_3)-d_2d_3\bar{w}_2\bar{w}_3)C_{2\theta}}\right] \tag{5.8}$$

where w_1, w_2, w_3 are weak measurement parameters on qubits 1, 2 and 3, respectively ($0 \leq w_1 \leq 1$, $0 \leq w_2 \leq 1$, and $0 \leq w_3 \leq 1$) and $\bar{w}_i = 1 - w_i$.

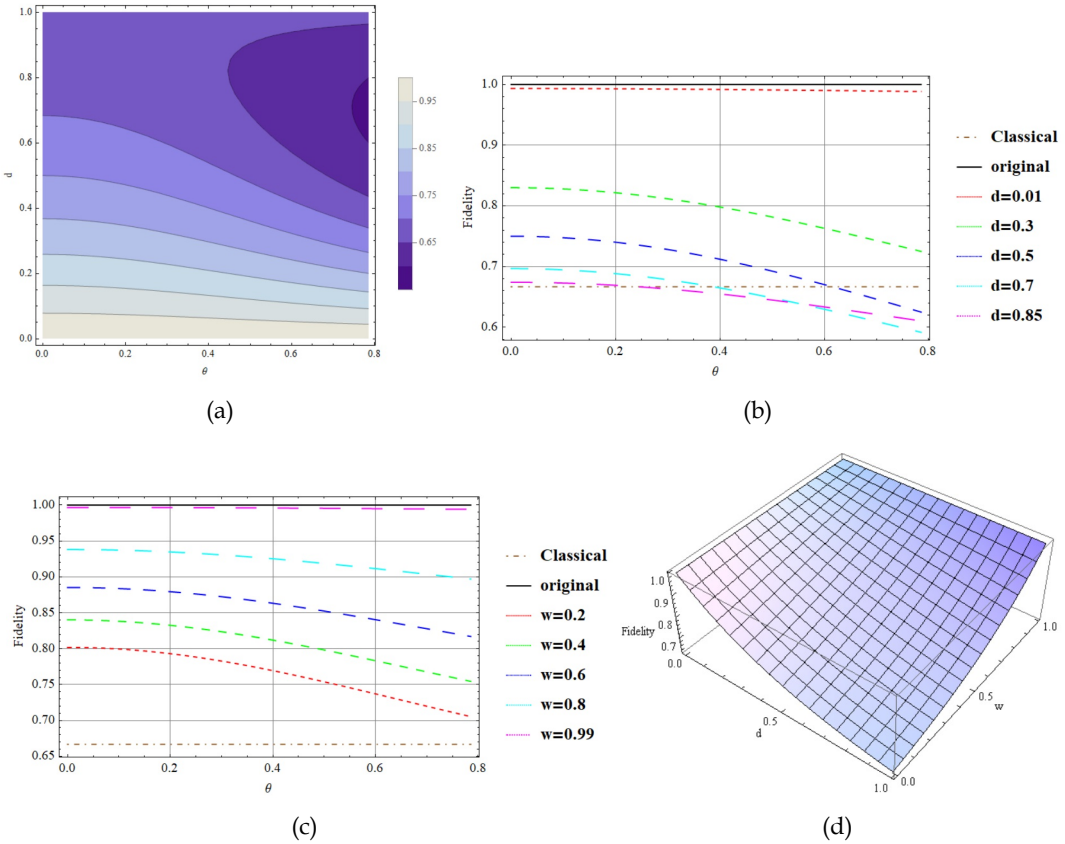


Figure 5.3 : Effects of decoherence and weak measurement on $|\Phi\rangle$ states: (a) and (b) represent loss of teleportation fidelity when all three qubits of $|\Phi\rangle$ states undergo decoherence ($d_1 = d_2 = d_3 = d$), (c) represents improvement in teleportation fidelity in decoherence environment ($d = 0.5$) using weak measurement on all three qubits of $|\Phi\rangle$ states ($w_1 = w_2 = w_3 = w$) and (d) represents effect of decoherence and weak measurement on $|\Phi\rangle$ state when $\theta = \frac{\pi}{8}$

Figure 5.3(c) demonstrates the effects of weak measurement and its reversal operations on the average fidelity under noisy conditions, considering d=0.5. A comparison of Figure 5.3(b)

and Figure 5.3(c) confirms the enhancement in teleportation fidelity at d=0.5 for the value of weak measurement strength, $w > 0.2$. For larger values of the weak measurement strength parameter, fidelity approaches 1 independent of the state parameter θ similar to the case of ideal conditions. This is incredible as one need not worry about decoherence and initial entanglement without compromising on the optimal efficiency of the protocol. Our results further reduce the constraints on an experimental set-up by providing flexibility to start the protocol with any partially entangled state even in presence of high decoherence. Clearly, the fidelity is always greater than $\frac{2}{3}$ even at higher decoherence values where the Svetlichny inequality is not violated by $|\Phi\rangle$ states. From Figure 5.3(c) and Figure 5.3(d), one can further conclude that partially entangled $|\Phi\rangle$ states are still more robust to decoherence under the applications of weak measurement and its reversal operations.

In order to further elaborate on reasons behind fidelity being $> \frac{2}{3}$ even at high decoherence where $|\Phi\rangle$ states fail to violate the Svetlichny inequality, we use global quantum discord [Rulli and Sarandy, 2011] to capture nonlocal correlations in the finally shared three-qubit mixed states. The quantum discord $D(\rho)$ for an arbitrary three-qubit state ρ_{ABC} under a set of local measurements $\{\Pi^k\}$ is defined as

$$D(\rho) = min_{\{\Pi^k\}}[S(\rho||\phi(\rho)) - S(\rho_A||\phi_A(\rho_A)) - S(\rho_B||\phi_B(\rho_B)) - S(\rho_C||\phi_C(\rho_C))] \tag{5.9}$$

where $\phi_i(\rho_i) = \sum_k \Pi^k \rho_i \Pi^k$ and $S(\rho)$ is von-Neumann entropy of the state ρ.

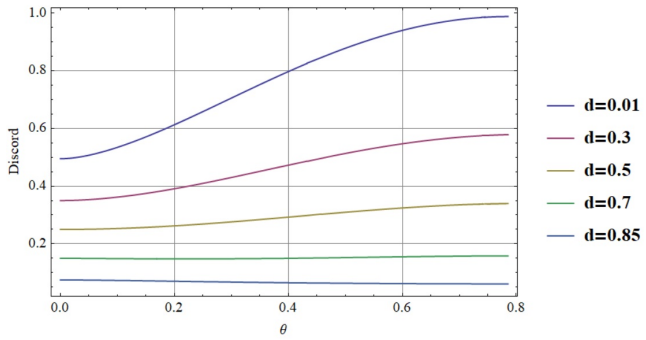


Figure 5.4 : Effects of decoherence on quantum correlations using discord for $|\Phi\rangle$ states

Figure 5.4 confirms that correlations in the $|\Phi\rangle$ states are much more robust in presence of decoherence as against the indications given by the Svetlichny inequality. The characterization of nonlocal correlations using discord and our modified operators, therefore, justifies the efficiency of $|\Phi\rangle$ states in quantum teleportation under real conditions.

$|GGHZ\rangle$ *states as quantum channels under real conditions*

In this sub-section, we consider three-qubit $|GGHZ\rangle$ states given by

$$|GGHZ\rangle = Cos\theta\,|000\rangle + Sin\theta\,|111\rangle \tag{5.10}$$

The quantum circuit for teleporting a single qubit using $|GGHZ\rangle$ states as quantum channels is

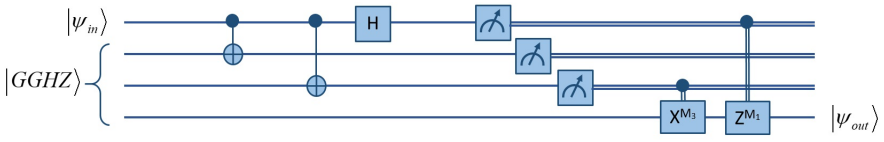


Figure 5.5 : A quantum circuit for teleportation using the $|GGHZ\rangle$ state as a quantum channel

shown in Figure 5.5 where the notations have standard representations as described earlier. Unlike $|\Phi\rangle$ states, the average teleportation fidelity using $|GGHZ\rangle$ states as resources in ideal conditions depends on the state parameter θ, i.e., $F_{avg} = \frac{1}{3}[2+Sin(2\theta)]$ which is the same as in [Karlsson and Bourennane, 1998]. Considering that we are interested in analyzing and comparing efficiencies of partially entangled three-qubit states under real conditions, the average teleportation fidelity under the influence of amplitude damping noise, and after applications of weak measurement and its reversal operations are evaluated as

$$F_{avg}^{(d)} = \frac{1}{6}\{4-(d_2+d_3-2d_2d_3)(1-C_{2\theta})+2\sqrt{\bar{d}_1}\sqrt{\bar{d}_2}\sqrt{\bar{d}_3}S_{2\theta}\} \tag{5.11}$$

and

$$F_{avg}^{(w)} = \frac{(1+d_1\bar{w}_1)(2+d_3\bar{w}_3d_2\bar{w}_2(1+2d_3\bar{w}_3))S_\theta^2+2C_\theta^2+S_{2\theta}}{3(C_\theta^2+(1+d_1\bar{w}_1)(1+d_2\bar{w}_2)(1+d_3\bar{w}_3)S_\theta^2)}, \tag{5.12}$$

respectively.

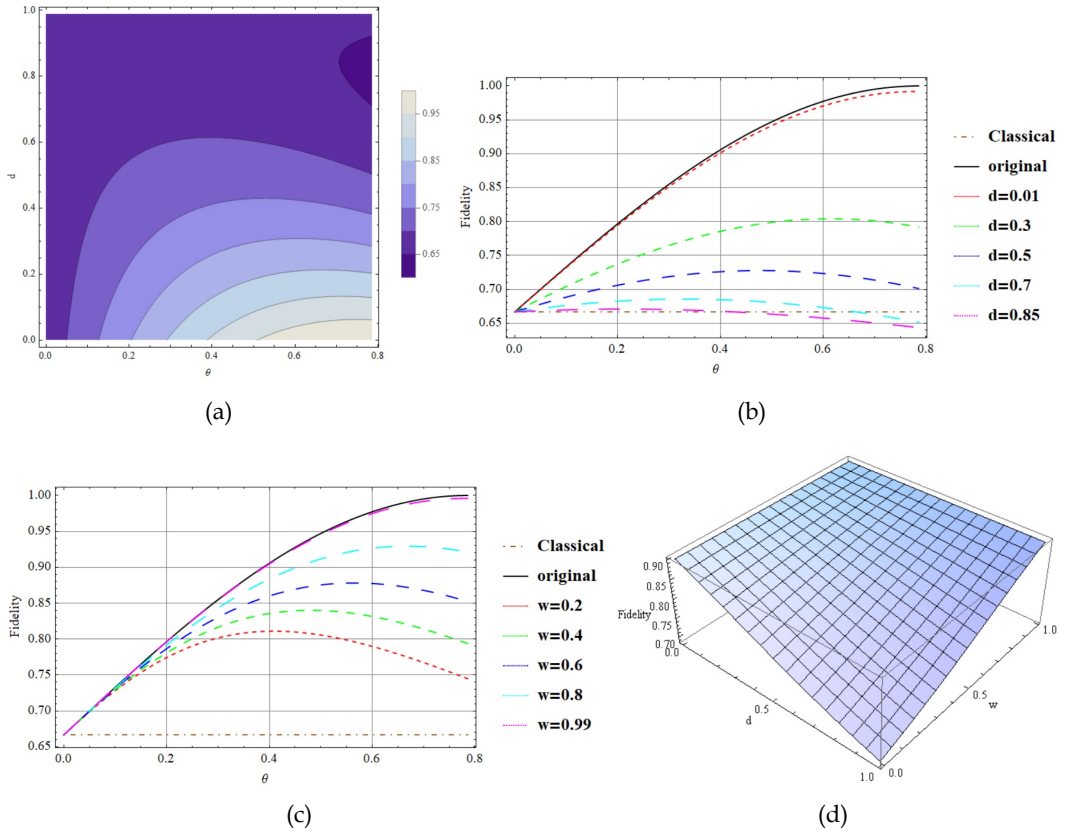


Figure 5.6 : Effects of decoherence and weak measurement on $|GGHZ\rangle$ states: (a) and (b) represent loss of teleportation fidelity when all three qubits of $|GGHZ\rangle$ states undergo decoherence $(d_1 = d_2 = d_3 = d)$, (c) represents improvement in teleportation fidelity in decoherence environment $(d = 0.5)$ using weak measurement on all three qubits of $|GGHZ\rangle$ states $(w_1 = w_2 = w_3 = w)$ and (d) represents effect of decoherence and weak measurement on $|GGHZ\rangle$ state when $\theta = \frac{\pi}{8}$

Figure 5.6(a) - Figure 5.6(d) depict effects of amplitude damping channels and weak measurement and its reversal operations on teleportation fidelity. Similar to the previous case, we observe that weak measurement and its reversal operations increase the teleportation fidelity for a given decoherence channel. In fact, for higher values of weak measurement strengths, one

can achieve fidelity equals to the one obtained in the ideal scenario. On the other hand, unlike the previous case, the maximally entangled states are found to be more robust under the influence of mild decoherence in comparison to partially entangled states. However, for higher decoherence, the robustness of partially entangled states towards teleportation fidelity increases with increase in the degree of entanglement and then decreases as one approaches the maximally entangled state. For a fixed noise parameter, similar observations can be obtained as one decreases the value of weak measurement strengths. Therefore, the properties and efficiencies of $|\Phi\rangle$ and $|GGHZ\rangle$ states in presence of noise and weak measurements are completely different from each other. A comparison of our results for efficiencies of $|\Phi\rangle$ and $|GGHZ\rangle$ states suggests that for lower values of state parameter θ, $|\Phi\rangle$ states are more robust to decoherence in comparison to the $|GGHZ\rangle$ states. The $|GGHZ\rangle$ states, however, may prove to be a better resource in terms of teleportation fidelity for higher values of θ. However, if the value of weak measurement parameter is 1 or close to 1, then the fidelity of $|\Phi\rangle$ states is unity- independent of the degree of entanglement in the initial resource- which is always greater than the one obtained using $|GGHZ\rangle$ states with the fidelity being equal for $\theta = \frac{\pi}{4}$ only. The above analysis further receives support from our discussions

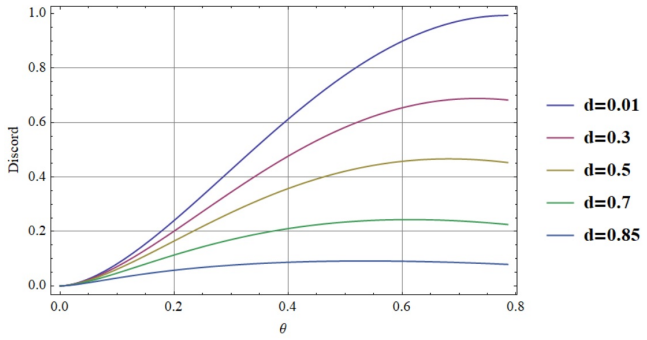


Figure 5.7 : Effects of decoherence on quantum correlations using discord for $|GGHZ\rangle$ states

of nonlocality using modified Mermin and Svetlichny operators in Chapter 3; and from Figure 5.4 and Figure 5.7 where the latter describes nonlocal correlations in originally prepared $|GGHZ\rangle$ states under different values of noise parameter.

$|W\rangle$ *states as quantum channels under real conditions*

Now, we consider another important class of three-qubit states as a quantum channel for teleportation, namely

$$|W\rangle = Sin\theta\,|001\rangle + Cos\theta(|100\rangle + |010\rangle)/\sqrt{2} \tag{5.13}$$

where if $\theta = 35.2644^{\circ}$, the state in Eq. (5.13) is a standard $|W\rangle$ state. In this case, Figure 5.8 describes the quantum circuit used for evaluating average teleportation fidelity. The quantum circuit in

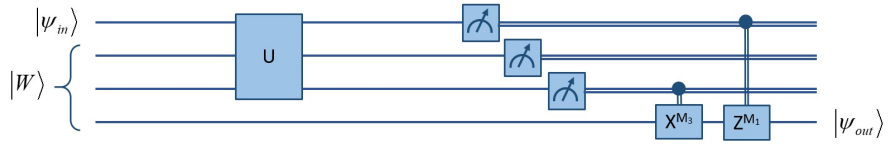


Figure 5.8 : A quantum circuit for teleportation using the $|W\rangle$ state as a quantum channel

Figure 5.8 [Jung *et al.*, 2008] is distinctly different from quantum circuits used for $|\Phi\rangle$ and $|GGHZ\rangle$ states. The unitary operation U is a three-qubit joint unitary operation and cannot be expressed in

terms of usual Pauli, Hadamard and C-NOT operations, such that

$$U = \frac{1}{2}\begin{bmatrix} 0 & 1 & 1 & 0 & \sqrt{2} & 0 & 0 & 0 \\ 0 & 0 & 0 & 2 & 0 & 0 & 0 & 0 \\ 0 & 0 & 0 & 0 & 0 & 0 & 0 & 2 \\ \sqrt{2} & 0 & 0 & 0 & 0 & 1 & 1 & 0 \\ 0 & 1 & 1 & 0 & -\sqrt{2} & 0 & 0 & 0 \\ 0 & \sqrt{2} & -\sqrt{2} & 0 & 0 & 0 & 0 & 0 \\ 0 & 0 & 0 & 0 & 0 & \sqrt{2} & -\sqrt{2} & 0 \\ \sqrt{2} & 0 & 0 & 0 & 0 & -1 & -1 & 0 \end{bmatrix}$$

Similar to the case of $|GGHZ\rangle$ states, teleportation fidelity in this case also depends on the state parameter θ, and can be given as $\frac{1}{3}[2 + Sin(2\theta)]$. In order to analyze effects of noise and weak measurements, we evaluate average fidelity using the circuit diagram in Figure 5.8 in presence of the amplitude damping noise and weak measurement operations such that

$$F_{avg}^{(d)} = \frac{1}{12}\{(6 - d_1 - d_2 + 2\sqrt{\bar{d}_1}\sqrt{\bar{d}_2})C_\theta^2 - 4(-2 + d_3)S_\theta^2 + 2(\sqrt{\bar{d}_1} + \sqrt{\bar{d}_2})\sqrt{\bar{d}_3}S_{2\theta}\} \tag{5.14}$$

and

$$F_{avg}^{(w)} = \frac{8 + d_1\bar{w}_1 + d_2\bar{w}_2 + 2d_3\bar{w}_3 + 4S_{2\theta} + (d_1\bar{w}_1 + d_2\bar{w}_2 - 2d_3\bar{w}_3)C_{2\theta}}{6((2 + d_1\bar{w}_1 + d_2\bar{w}_2)C_\theta^2 + 2(1 + d_3\bar{w}_3)S_\theta^2)}, \tag{5.15}$$

respectively.

In contrast to $|\Phi\rangle$ and $|GGHZ\rangle$ states, teleportation fidelity using standard $|W\rangle$ state is always more in comparison to the use of other partially entangled $|W\rangle$ states as shown in Figure 5.9(a) and Figure 5.9(b) irrespective of the value of noise parameter. Moreover, for $d \geq 0.5$, the set of $|W\rangle$ states are not useful for quantum teleportation. However, as demonstrated in Figure 5.9(c), average fidelity clearly exceeds the classical bound in presence of weak measurements techniques even if $d = 0.5$ for certain ranges of the state parameter θ, and therefore using weak measurement and its reversal operations $|W\rangle$ states can also be seen as useful resources for quantum teleportation. Our results show that $|\Phi\rangle$ and $|GGHZ\rangle$ states are more robust against noise in comparison to the use of $|W\rangle$ states both in absence and presence of weak measurement and its reversal operations. However, for small values of the weak measurement parameter, we surprisingly find that the standard $|W\rangle$ state is more efficient than the $|\Phi\rangle$ and $|GGHZ\rangle$ states for the same value of the state parameter, i.e. at $\theta = 35.2644^\circ$. Although the ranges of θ and weak measurement parameter for which $|W\rangle$ states are more efficient in comparison to $|\Phi\rangle$ and $|GGHZ\rangle$ states are very small, the result, nevertheless, is of high significance and further indicates towards complexity of nonlocal correlations. Moreover, for higher values of weak measurement parameter, the standard $|W\rangle$ state leads to a fidelity very close to unity even in presence of high decoherence which is contrary to our experience of standard $|W\rangle$ states leading to probabilistic results with fidelity depending on the parameters of the input state to be teleported [Shi and Tomita, 2002]. Further, in contrast to the Svetlichny inequality which suggests $|W\rangle$ states to be highly vulnerably to decoherence, nonlocal correlations in $|W\rangle$ states, as shown by global discord and our modified operators, are much more robust even in presence of high decoherence.

$|W_n\rangle$ *states as quantum channels under real conditions*

Finally, we consider another important set of three-qubit states as a quantum channel for teleportation, namely

$$|W_n\rangle = \frac{1}{\sqrt{2+2n}}\left[|001\rangle + \sqrt{n}|100\rangle + \sqrt{n+1}|010\rangle\right] \tag{5.16}$$

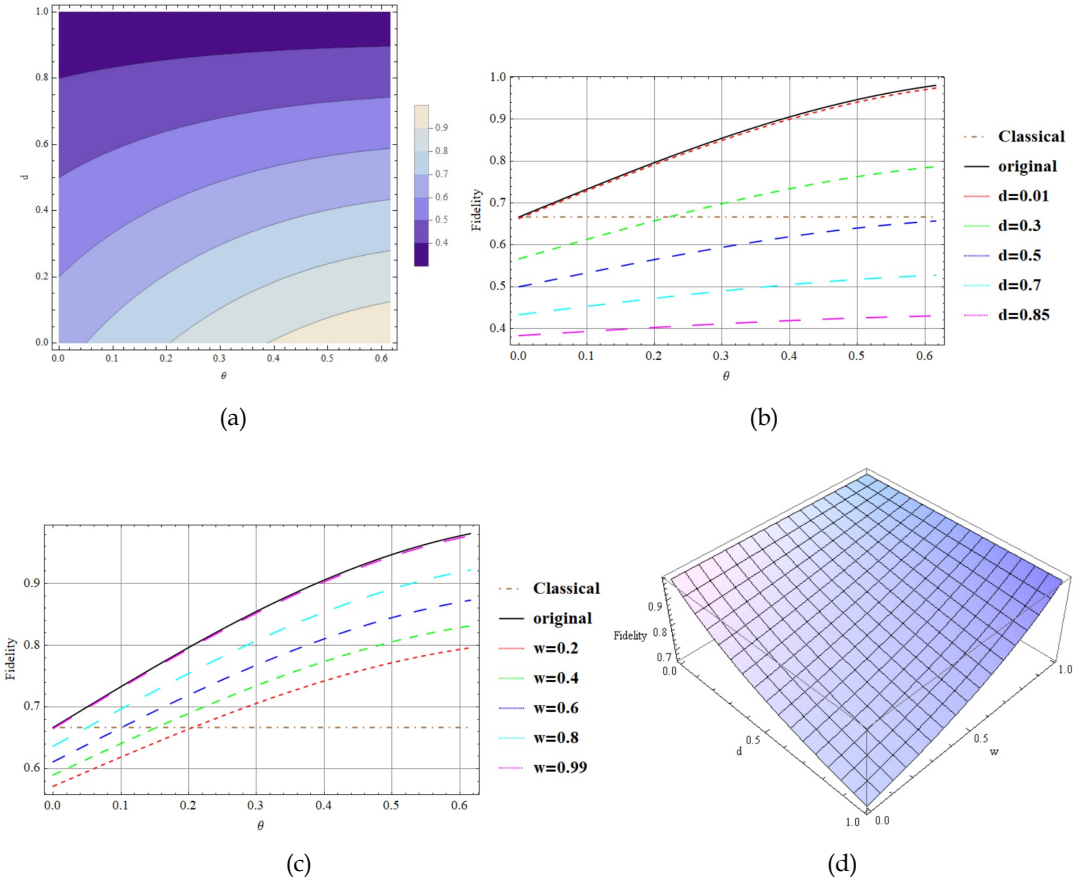


Figure 5.9 : Effects of decoherence and weak measurement on the $|W\rangle$ states: (a) and (b) represent loss of teleportation fidelity when all three qubits of $|W\rangle$ states undergo decoherence ($d_1 = d_2 = d_3 = d$), (c) represents improvement in teleportation fidelity in decoherence environment ($d = 0.5$) using weak measurement on all three qubits of $|W\rangle$ states ($w_1 = w_2 = w_3 = w$) and (d) represents effect of decoherence and weak measurement on standard $|W\rangle$ state (i.e. $\theta = 35.2644^\circ$ or $0.6155 rad$)

The quantum circuit used for evaluating average teleportation fidelity using $|W_n\rangle$ states is the same as that for $|W\rangle$ states, given in Figure 5.8. Similar to the case of $|GGHZ\rangle$ and $|W\rangle$ states, teleportation fidelity in this case also depends on the state parameter n, and given as

$$F_{avg} = \frac{7(1+n)+2\sqrt{2(1+n)}+2\sqrt{n}(1+\sqrt{2(1+n)})}{12(1+n)} \tag{5.17}$$

Using the circuit diagram in Figure 5.8, the average teleportation fidelity under the influence of amplitude damping noise, and after the applications of weak measurement and its reversal operations are evaluated as

$$F_{avg}^{(d)} = \frac{7(1+n)-d_1-nd_2+2\sqrt{2(1+n)\bar{d}_1\bar{d}_3}-2d_3(1+n)+2\sqrt{n\bar{d}_2}\left(\sqrt{\bar{d}_1}+\sqrt{2(1+n)\bar{d}_3}\right)}{12(1+n)} \tag{5.18}$$

and

$$F_{avg}^{(w)} = \frac{7(1+n)+2\sqrt{n}+2\sqrt{2(1+n)}+2\sqrt{2n(1+n)}+2d_1\bar{w}_1+2nd_2\bar{w}_2+2(1+n)d_3\bar{w}_3}{6\,(2+2n+d_1\bar{w}_1+nd_2\bar{w}_2+(1+n)d_3\bar{w}_3)}, \tag{5.19}$$

respectively.

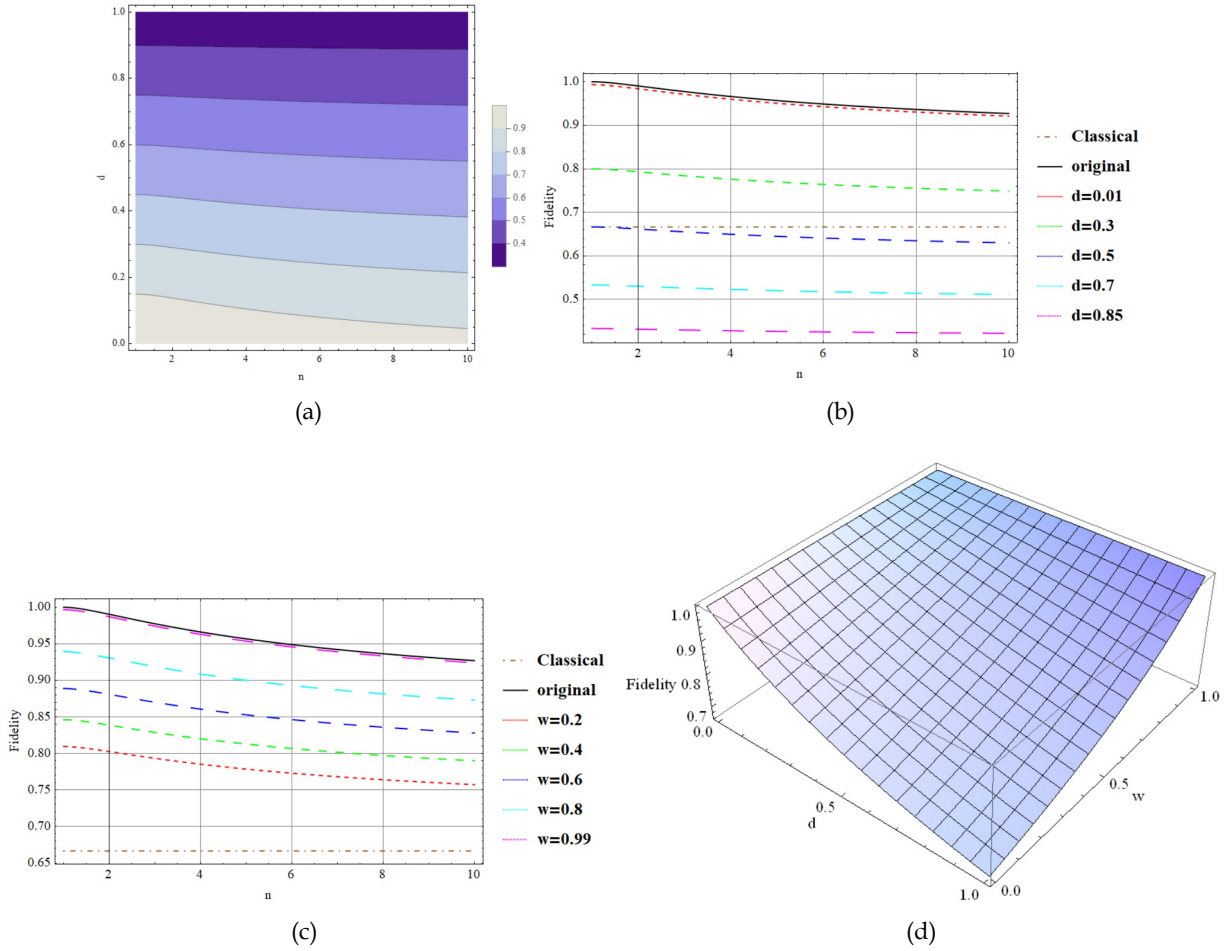
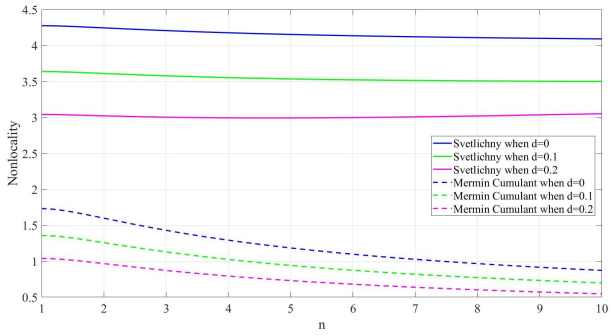


Figure 5.10 : Effects of decoherence and weak measurement on the $|W_n\rangle$ states: (a) and (b) represent loss of teleportation fidelity when all three qubits of $|W_n\rangle$ states undergo decoherence ($d_1 = d_2 = d_3 = d$), (c) represents improvement in teleportation fidelity in decoherence environment ($d = 0.5$) using weak measurement on all three qubits of $|W_n\rangle$ states ($w_1 = w_2 = w_3 = w$) and (d) represents effect of decoherence and weak measurement on $|W_1\rangle$ state

Figure 5.10(a) - Figure 5.10(c) illustrate effects of amplitude damping channel and weak measurement and its reversal operations on teleportation fidelity for $|W_n\rangle$ states. Figure 5.10(b) shows that for controlled teleportation, $|W_n\rangle$ states are fairly robust against the presence of noise in comparison to $|W\rangle$ states. In fact, the fidelity falls below the classical limit only if the decoherence parameter is close to 0.5. Similar to the previous cases, the application of weak measurement and its reversal operations reduces the effects of decoherence channel on teleportation fidelity and results in fidelity obtained under ideal scenario, for weak measurement parameter being close to 1. In comparison to all $|W_n\rangle$ states, the fidelity of $|W_1\rangle$ state is maximum in ideal as well as in noisy condition with the application of weak measurements. Figure 5.10(d) represents effects of decoherence and weak measurements on teleportation fidelity using the $|W_1\rangle$ state. Our results further demonstrate that for $w = 1$, the fidelity using $|W_1\rangle$ states is always unit irrespective of the value of decoherence parameter. Clearly, one can always find a set of $|W_n\rangle$ states leading to better fidelity than $|W\rangle$ states at least for lower values of the state parameter n. Although Svetlichny inequality shows the absence of nonlocal correlations even for very mild decoherence, Mermin-cumulant inequality and discord confirm the existence of nonlocal correlations in the presence of noise as shown in Figure 5.11.



(a)

Figure 5.11 : Effects of decoherence on quantum correlations of $|W_n\rangle$ states using Svetlichny and Mermin-cumulant inequalities

5.4 QUANTUM DENSE CODING

Bennett and Wiesner [Bennett and Wiesner, 1992] proposed one of the simplest applications of quantum entanglement in the form of a dense coding protocol. Classically, by manipulating the state of a single bit, a sender can communicate one bit of information to a receiver. However, if a sender and a receiver share a maximally entangled state of two qubits, then the sender can communicate two bits of classical message to the receiver by locally manipulating his/her one qubit. Therefore, use of N pairs of maximally entangled two-qubit states results in the transmission of 2N bits of information, thereby doubling the classical information capacity of a channel. In the superdense coding protocol, an entangled state is distributed between a sender and a receiver. The sender performs one of the four single-qubit unitary operations, i.e., I, σ_x, σ_{iy} and σ_z, based on a prior agreed encoding scheme and information that he/she wants to communicate to the sender. Once the encoding is performed, the sender sends his/her qubit to the receiver, who in turn performs a two-qubit Bell-state measurement to decode the message.
The dense coding capacity [Bowen, 2001] for a quantum system ρ_{AB} can be used as a measure of its efficiency to transmit classical information, and is given by

$$C = log_2(D_A) + S(\rho_B) - S(\rho_{AB}) \tag{5.20}$$

where D_A is the dimension of Alice's sub-system, $S(\rho)$ is von-Neumann entropy of the state ρ such that qubit A is with Alice and B is with Bob.

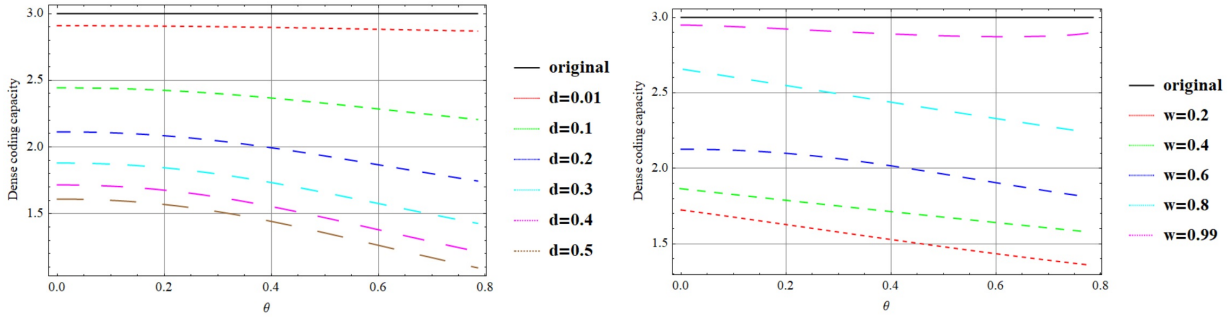
5.4.1 Three qubit states as quantum channels for dense coding

For analyzing efficiencies of partially entangled three-qubit states for dense coding protocol, we assume that first two qubits are with Alice and the last qubit is with Bob. For a maximally entangled $|\Phi\rangle$ or $|GHZ\rangle$ state, Alice can send 3 bits of classical information as she can in principle generate eight distinct orthogonal basis states by performing eight different operations on her two qubits. However, for the standard $|W\rangle$ state as a quantum channel, Alice can only send 2.91831 bits of information to Bob. We now proceed to analyze how the efficiencies of different partially entangled states stand for the dense coding protocol.

$|\Phi\rangle$ *state as a quantum channel*

Using Eq. (5.20), we find that the dense coding capacity using $|\Phi\rangle$ state as a quantum channel is 3 bits. This indicates that in ideal conditions, one can use any of the $|\Phi\rangle$ states for maximum information transfer irrespective of the degree of entanglement of the input state. For actual evaluation, using the amplitude damping channel similar to the teleportation case, the dense coding capacity of $|\Phi\rangle$ states decreases in noisy conditions (see Figure 5.12(a)). For example, $|\Phi\rangle$

states are not useful for dense coding protocol for $d > 0.2$. Figure 5.12(b) demonstrates the effects of weak measurement and its reversal operations on the dense coding capacity, considering $d = 0.5$. Clearly, the dense coding capacity exceeds the classical bound whenever $w \geq 0.6$ for a given range of state parameters. At higher values of w, the dense coding capacity is always better than the classical one. The increase in dense coding capacity, however, decreases with the value of state parameter indicating that if the originally prepared states are less entangled one will obtain better results in dense coding protocol in noisy conditions. Therefore, the effects of decoherence on dense coding protocol in absence or presence of weak measurement techniques using $|\Phi\rangle$ states are much more pronounced in comparison to teleportation protocol.



(a) (b)

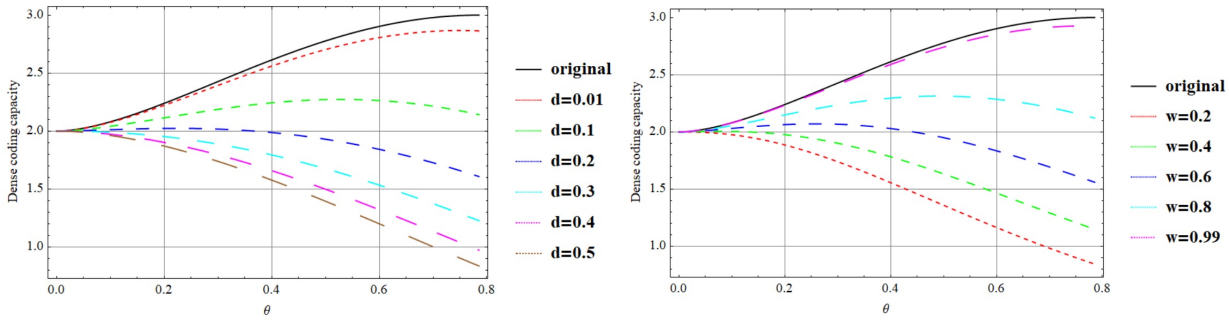
Figure 5.12 : Effects of decoherence and weak measurement on $|\Phi\rangle$ states: (a) represents loss of dense coding capacity when all three qubits of $|\Phi\rangle$ states undergo decoherence ($d_1 = d_2 = d_3 = d$), (b) represents improvement in dense coding capacity in decoherence environment ($d = 0.5$) using weak measurement on all three qubits of $|\Phi\rangle$ states ($w_1 = w_2 = w_3 = w$)

$|GGHZ\rangle$ *state as a quantum channel*

The dense coding capacity of $|GGHZ\rangle$ states as resources in ideal condition is given as

$$C = log_2(4) - Cos^2\theta log_2(Cos^2\theta) - Sin^2\theta log_2(Sin^2\theta) \tag{5.21}$$

Similar to the teleportation case and unlike the $|\Phi\rangle$ states where dense coding capacity is independent of the state parameter, here the channel capacity depends on the state parameter and increases with the increase in degree of entanglement of the input state. Figure 5.13(a) and Figure 5.13(b) describe effect of amplitude damping channel and weak measurement and its reversal operations on dense coding capacity, respectively. Similar to the $|\Phi\rangle$ states, in the decoherence environment, the dense coding capacity falls below the classical limit for $d \geq 0.2$. On applications of weak measurement and its reversal operations, the dense coding capacity regains its quantum advantages for $w \geq 0.6$. Clearly, the impact of decoherence on dense coding capacity is much more adverse as compared to its effect on average fidelity. Moreover, similar to the teleportation scenario, in this case also, the dense coding capacity above classical bound increases with the state parameter, attains a maximum value and then decreases again. Similarly, if we compare the efficiencies of $|\Phi\rangle$ and $|GGHZ\rangle$ states in noisy conditions, we found that for lower (higher) values of the state parameter θ, $|\Phi\rangle$ ($|GGHZ\rangle$) states are more robust in comparison to $|GGHZ\rangle$ ($|\Phi\rangle$) states. For example, if we consider decoherence parameter $d = 0.5$, then for $\theta \leq 0.54$, $|\Phi\rangle$ states are better resources than $|GGHZ\rangle$ states and for $\theta > 0.54$, $|GGHZ\rangle$ states are better resources than $|\Phi\rangle$ states.



(a) (b)

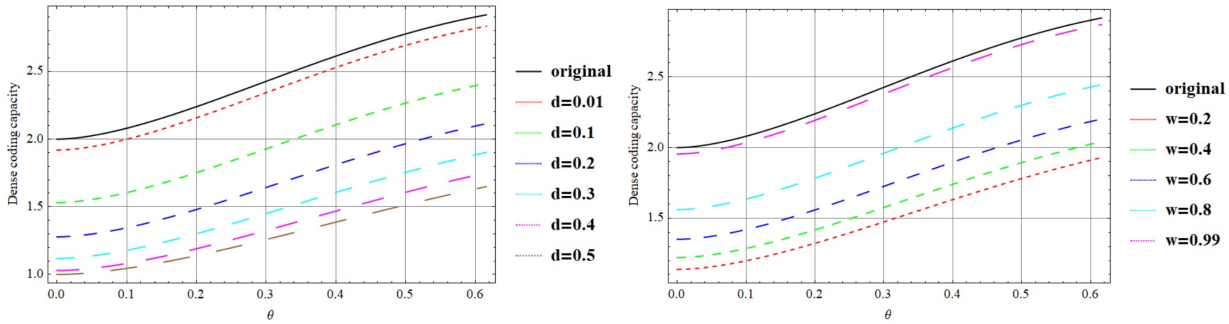
Figure 5.13 : Effects of decoherence and weak measurement on $|GGHZ\rangle$ states: (a) represents loss of dense coding capacity when all three qubits of $|GGHZ\rangle$ states undergo decoherence $(d_1 = d_2 = d_3 = d)$, (b) represents improvement in dense coding capacity in decoherence environment $(d = 0.5)$ using weak measurement on all three qubits of $|GGHZ\rangle$ states $(w_1 = w_2 = w_3 = w)$

$|W\rangle$ *state as a quantum channel*

Using $|W\rangle$ states as quantum channels, the dense coding capacity is given by

$$C = log_2(4) - Cos^2\theta log_2(Cos^2\theta) - Sin^2\theta log_2(Sin^2\theta) \tag{5.22}$$

The dense coding capacity has exactly the same expression as for the $|GGHZ\rangle$ states in ideal



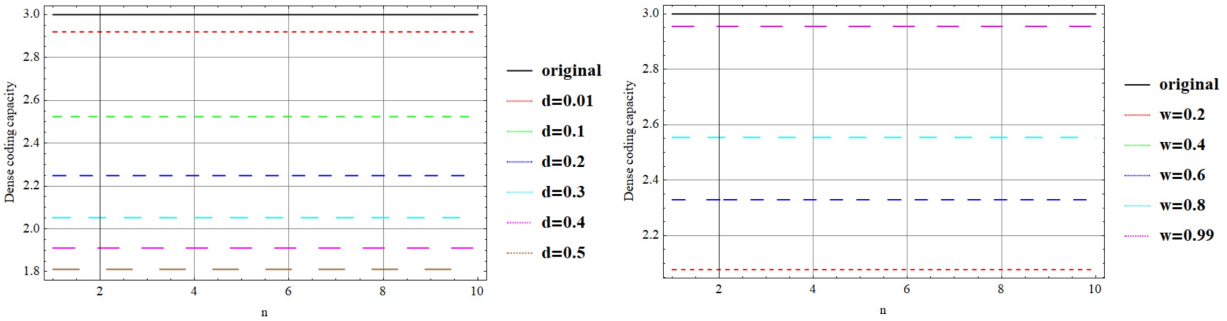
(a) (b)

Figure 5.14 : Effects of decoherence and weak measurement on $|W\rangle$ states: (a) represents loss of dense coding capacity when all three qubits of $|W\rangle$ states undergo decoherence $(d_1 = d_2 = d_3 = d)$, (b) represents improvement in dense coding capacity in decoherence environment $(d = 0.5)$ using weak measurement on all three qubits of $|W\rangle$ states $(w_1 = w_2 = w_3 = w)$

conditions. Figure 5.14(a) and Figure 5.14(b) describe effects of amplitude damping decoherence and weak measurement and its reversal operations on the dense coding capacity using $|W\rangle$ states as a quantum channel. A comparison of dense coding efficiencies for the three states indicates that $|\Phi\rangle$ and $|GGHZ\rangle$ states are more robust towards noise for the dense coding protocol in comparison to $|W\rangle$ states. Within the class of $|W\rangle$ states, weak measurements and its reversal operations enhance the dense coding capacity and it increases with the state parameter as well. Similar to teleportation, at $\theta = 35.2644°$, the standard $|W\rangle$ states are more efficient than $|\Phi\rangle$ and $|GGHZ\rangle$ states for certain values of the weak measurement parameter (say $w = 0.6$). Nevertheless, for all three states the efficiency of teleportation shows more resistance to the amplitude damping noise than the efficiency of dense coding protocol.

$|W_n\rangle$ state as a quantum channel

Using $|W_n\rangle$ states as resources, the dense coding capacity is 3 bits, suggesting that any of the $|W_n\rangle$ states can be used to transfer maximum information between a sender and a receiver. Unlike $|W\rangle$ states, where the dense coding capacity depends on the state parameter, the amount of information transferred using $|W_n\rangle$ states is independent of the state parameter. In fact, the channel capacity in ideal conditions is equivalent to that of $|\Phi\rangle$ states. Although the dense coding capacity reduces in noisy conditions, it surprisingly remains same for the complete set of $|W_n\rangle$ states independent of the state parameter $(1 \leq n \leq 10)$. Figure 5.15(a) suggests that for $d > 0.31$, dense coding capacity goes below the classical limit. Interestingly, the channel capacity obtained for any value of d is better than the one obtained using other partially entangled three-qubit states as inputs. With the application of weak measurement and its reversal operations, $|W_n\rangle$ states lead to dense coding capacity greater than the classical limit, even for lower values of weak measurement parameter.



(a) (b)

Figure 5.15 : Effects of decoherence and weak measurement on channel capacity of $|W_n\rangle$ states: (a) represents reduction of dense coding capacity when all three qubits of $|W_n\rangle$ state undergo decoherence $(d_1 = d_2 = d_3 = d)$, (b) represents improvement in dense coding capacity in decoherence environment $(d = 0.5)$ using weak measurement on all three qubits of $|W_n\rangle$ states $(w_1 = w_2 = w_3 = w)$

5.5 EFFICIENCY OF PARTIALLY ENTANGLED STATES IN NOISY CONDITIONS USING NON-OPTIMUM WEAK MEASUREMENT OPERATIONS

In the previous section, we used the optimum value of weak measurement reversal strength, which leads to the effective enhancement in the efficiencies of quantum information processing protocols, as described in Chapter 1 given by $w_r = w + d(1-w)$ [Kim *et al.*, 2012].
In this section, we raise the question of using non-optimal weak measurement reversal operations, namely, *Is it possible to obtain better efficiency in a protocol using non-optimal reversal operations in comparison to the use of optimal reversal operations*? Interestingly, our results show that in case of $|GGHZ\rangle$ states, for a given decoherence parameter, fixing the value of weak measurement parameter (or w_r) results in the fidelity (or dense coding capacity) to be equal to the fidelity (or dense coding capacity) which can be obtained using a maximally entangled pure state. For example, using $|GGHZ\rangle$ states as a quantum channel, at $d = 0.5$ and $w = 0.8$, one can achieve fidelity close to unity for the values of $w_r = 0.99$ and $\theta = 0.029$ (Figure 5.16(a) and Figure 5.16(b)). In addition, if we first fix $w_r = 0.99$, then for the value of decoherence parameter $d = 0.5$, use of partially entangled $|GGHZ\rangle$ states as resources result in very high average teleportation fidelity at very small values of state parameter $(\theta \in [0.003, 0.4])$, for all values of weak measurement strength below $w = 0.98$. Similarly, for dense coding protocol also one can transfer 2.87 bits of message using Alice's 2 qubits for same values of parameters (Figure 5.16(c) and Figure 5.16(d)).

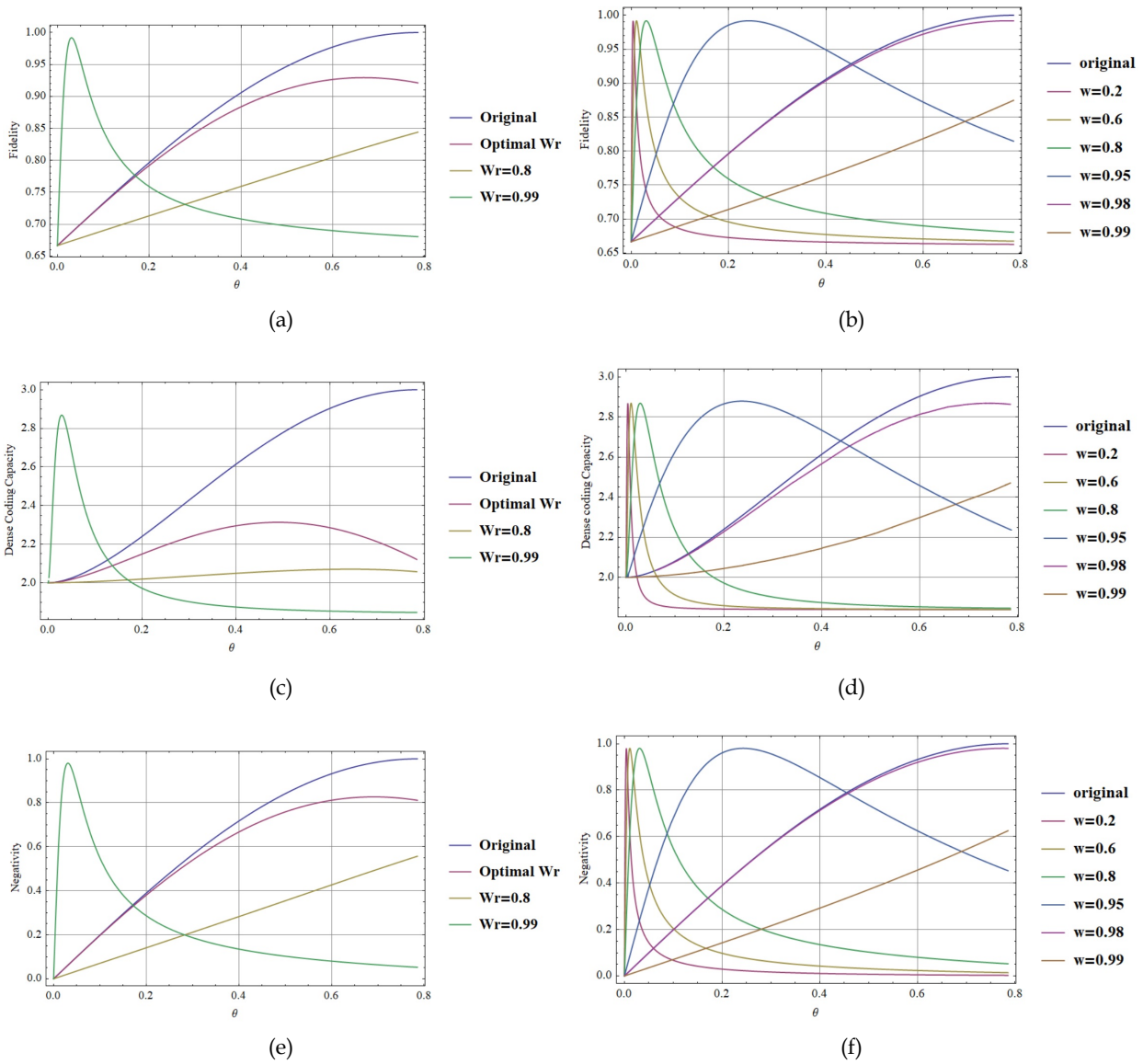


Figure 5.16 : (a) Average teleportation fidelity, (c) dense coding capacity, (e) negativity for $|GGHZ\rangle$ states when decoherence parameter $d = 0.5$ and weak measurement strength $w = 0.8$; and (b) Average teleportation fidelity, (d) dense coding capacity, (f) negativity for $|GGHZ\rangle$ states when decoherence parameter $d = 0.5$ and reversal weak measurement strength $w_r = 0.99$

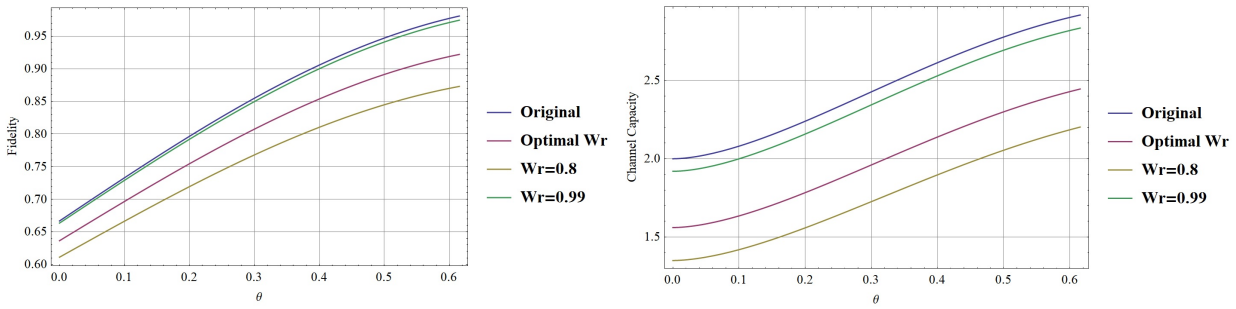
For studying the efficiencies of mixed states evolving from the initially prepared $|GGHZ\rangle$ states for non-optimal weak measurement strengths at different values of state parameters, we characterize the degree of entanglement in these states using tripartite negativity [Sabín and García-Alcaine, 2008], as a measure of entanglement for mixed states, which is defined as

$$N(\rho_{ABC}) = \sqrt[3]{N(\rho^{T_A})N(\rho^{T_B})N(\rho^{T_C})} \tag{5.23}$$

where $N(\rho^{T_i}) = -2\lambda_{neg}$, λ_{neg} is sum of negative eigenvalues of ρ^{T_i}, and ρ^{T_i} is partial transpose of ρ_{ABC} with respect to the sub-system i. Clearly for $\theta = 0.029$, the value for tripartite negativity is very high (see Figure 5.16(e) and Figure 5.16(f)), therefore, the degree of entanglement of the finally shared state further justifies the efficiencies of these states at lower value of the state parameter. In case of $|\Phi\rangle$ states using $w_r = 0.92$ and $\theta > 0.5$, for fixed $d = 0.5$ and $w = 0.8$, one can obtain greater fidelity than the one obtained using optimal relation between parameters used in the protocol. In

fact, one can obtain greater fidelity than the optimal case for any decoherence at least for some range of the state parameter.

In case of $|W\rangle$ states, one can achieve better fidelity (or dense coding capacity) using non-optimal reversal operations in comparison to the use of optimal reversal operations used in the protocol. Figure 5.17(a) and Figure 5.17(b) show that at $d = 0.5$ and $w = 0.8$, the fidelity and dense coding capacity are greater at $w_r = 0.99$ in comparison to the one achieved with optimal reversal weak measurements and close to the one obtained in ideal situations. In case of $|W_n\rangle$ states, non-optimal reversal measurements result in same observations as that in the case of $|W\rangle$ states for both the protocols.



(a) (b)

Figure 5.17 : (a) Average teleportation fidelity, (b) dense coding capacity for $|W\rangle$ states at $d = 0.5$ and $w = 0.8$

5.6 SUMMARY

In any quantum information processing protocol, it is imperative to analyze efficacy of entangled resources under real conditions. In fact, in any actual set-up, avoiding interaction of qubits with the environment may not be feasible, hence, one needs to study models that lead to real conditions such that maximum efficiency can be achieved and associated parameters and their effects on the protocol can be understood. Therefore, the present chapter analyzed efficiencies of three-qubit partially entangled states in two inequivalent classes of three-qubit entangled states in presence of noise and applications of weak measurement and its reversal operations. The results indicate that, for teleportation protocol, $|\Phi\rangle$ states are more robust to decoherence for smaller values of parameter θ in comparison to the $|GGHZ\rangle$ states. However, the efficiency of $|GGHZ\rangle$ states exceeds that of $|\Phi\rangle$ states once θ exceeds a certain value. For example, when decoherence is 0.5 and state parameter $\theta \leq \frac{\pi}{9}(= 0.35)$, the $|\Phi\rangle$ states are more efficient for teleportation in comparison to $|GGHZ\rangle$ states, whereas for $\theta > \frac{\pi}{9}$, $|GGHZ\rangle$ states are more efficient. Moreover, in general, efficiencies of $|\Phi\rangle$ and $|GGHZ\rangle$ states are found to be more robust in comparison to $|W\rangle$ and $|W_n\rangle$ states in presence of noise. In all four cases, the fidelity of teleportation increases with the strength of weak measurement and its reversal operations irrespective of the value of decoherence parameter. For dense coding protocol, similar results were found, i.e., degradation in dense coding capacity with increase in decoherence and enhancement in capacity with applications of weak measurement and its reversal operations. The efficiencies of these states are shown to be justified in view of the robustness of nonlocal correlations as characterized using the Svetlichny operator, our modified operators and global quantum discord. The states are found to be efficient for controlled communication protocols even in the regions where the Svetlichny inequality is not violated by these states in presence and absence of noise. Interestingly, nonlocal correlations as identified by the geometric discord and modified Mermin inequality for a given range of theta are always more for a maximally entangled input state, the efficiency of initially prepared partially entangled $|\Phi\rangle$ or $|GGHZ\rangle$ states for teleportation and dense coding is found to be better than the efficiency

of maximally entangled states in presence of noise. Therefore, in contrast to the general belief that more correlations in the input state may lead to better efficiency, this study found that less correlations in input state can be more useful for certain protocols- provides another proof towards the complex nature of multi-qubit entanglement, nonlocality and associated efficiency. The results also indicate that, for a specific value of state parameter θ, when non-optimum reversing weak measurement were applied, the partially entangled $|GGHZ\rangle$ states are more efficient for quantum protocols than all other states of the same class. In fact, we found that even if the input state is close to a product state, applications of weak measurement and reversal operations may lead to an optimal efficiency. Whereas in case of $|W\rangle$ states, with non-optimum weak measurement reversal operations also the standard $|W\rangle$ state is more efficient in comparison to partially entangled states of the same set. Hence, the study presented in this chapter provides an efficient analysis to select appropriate entangled resources for quantum information processing protocols depending on the decoherence parameter as well as the weak measurement and its reversal strength parameter.

Further, with each additional qubit, the number of participants in a quantum information processing protocol can be added. Therefore, it is also important to consider efficiencies of multi-qubit partially entangled states in different quantum communication protocols. Hence, the next chapter is dedicated to addressing the use of $N+2$-qubit partially entangled multiqubit states for controlled protocols, which includes $N+2$ number of participants consisting a sender, a receiver and N controllers.

...